stichting
mathematisch
centrum

MC

AFDELING TOEGEPASTE WISKUNDE
(DEPARTMENT OF APPLIED MATHEMATICS)

TW 246/83 OKTOBER

H.A. LAUWERIER

LOCAL BIFURCATION OF A LOGISTIC DELAY MAP

kruislaan 413 1098 SJ amsterdam

Printed at the Mathematical Centre, Kruislaan 413, Amsterdam, The Netherlands.

The Mathematical Centre, founded 11 February 1946, is a non-profit institution for the promotion of pure and applied mathematics and computer science. It is sponsored by the Netherlands Government through the Netherlands Organization for the Advancement of Pure Research (Z.W.O.).

1980 Mathematics subject classification: 58F14, 39A10, 14E07

Local bifurcation of a logistic delay map

by

H.A. Lauwerier

ABSTRACT

The difference equation $x_{n+1} = ax_n(1-(1-b)x_n-bx_{n-1})$ is considered as an iterative Cremona transformation in the projective plane. Only local bifurcation phenomena are considered here. It is shown how the theory of normal forms can be used to explain or predict what can be seen on a personal computer with a visual display. In a set of Appendices the technique of the normal forms is given with an application to a quadratic map of the kind

$$x' = y, \quad y' = Ax + By + Cx^2 + Dxy + Ey^2.$$

Explicit formulas are given for the shape and the size of the Hopf ellipse and for the axis of the Arnold forms at weak resonance points.

KEY WORDS & PHRASES: *logistic delay map; bifurcation; non-linear difference equations; normal forms; cremona transformation*

1. INTRODUCTION

In this report we consider some aspects of the bifurcation behaviour of the planar map

$$(1.1) \qquad \begin{cases} x' = y, \\ y' = ay(1-bx-(1-b)y), \end{cases}$$

where $0 \leq a \leq 5$, $0 \leq b \leq 1$. This map is equivalent to a family of logistic difference equations containing a delay term

$$(1.2) \qquad x_{n+1} = ax_n(1-(1-b)x_n-bx_{n-1}).$$

The extreme cases $b = 0$ and $b = 1$ are the well-known model due to May and the model studied by ROGERS & POUNDERS [1] and by ARONSON et al. [2].

As a generalisation of (1.1) we may consider the quadratic map

$$(1.3) \qquad \begin{cases} x' = y, \\ y' = Ax + By + Cx^2 + Dxy + Ey^2, \end{cases}$$

essentially a 4-parameter map.

Here we consider mainly local bifurcation properties. The topics are Hopf bifurcation, resonance phenomena, Arnold horns. The theory is those of normal forms. Since the technique of normal forms is hardly available in an easily applicable form we have collected the most important results at the end of this report. In Appendix A we show how the normal form

$$(1.4) \qquad w = \lambda z - Qz^2\bar{z} + \ldots$$

for bifurcation at the origin can be obtained excluding the cases 1 : 3 and 1 : 4 of strong resonance. This means that

$$(1.5) \qquad \lambda = (1+\mu)e^{i\alpha}$$

with $\alpha \neq 2\pi/3, \pi/2$.

In Appendix B we give the relevant theory of Hopf bifurcation and weak resonance. The only thing that matters is the value of Q for $\mu = 0$. The radius of the Hopf circle is given by

$$\mu/R^2 = \mathrm{Re}(e^{-i\alpha}Q). \tag{1.6}$$

The axis of the Arnold horn in the λ-plane is given by (cf. fig. 1.1)

$$\phi = \arg(e^{-i\alpha}Q). \tag{1.7}$$

The important case of strong resonance 1 : 4 has been considered in a previous report [3].

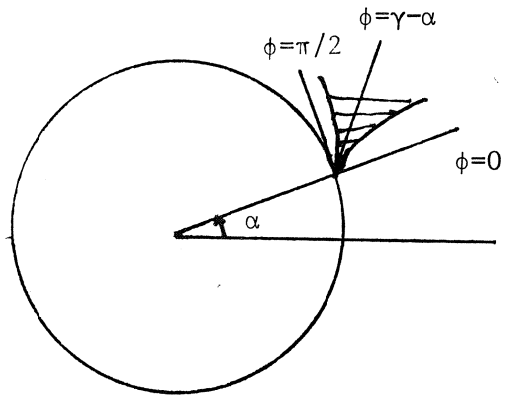

Fig. 1.1. Arnold horn at weak reasonance

In Appendix C the theory of normal forms is applied to the general map (1.3) with respect to the fixed point at the origin. This gives a Hopf ellipse with the equation

$$x^2 - 2xy\cos\alpha + y^2 = R^2 \tag{1.8}$$

where R is given by (1.6).

In section 2 we consider the elementary properties of the map (1.1) and in particular the nature of its fixed points, the shape of the Hopf ellipse etcetera. In section 3 we consider the same map as a particular case of a Cremona transformation in the projective plane. This may help us to understand the behaviour of the map outside the natural domain $x > 0$, $y > 0$.

In this study the guiding-principle has always been to obtain full understanding of the phenomena revealed by a (personal) computer with a visual display and to be able to predict the outcome of computer experiments If the bifurcation parameter μ is sufficiently small theory and experiment are in perfect agreement. However, there are situations where $\mu = 0.1$ is small and situations where $\mu = 0.01$ is large. In section 4 we discuss a number of computer experiments for such values of μ.

In a subsequent publication a few aspects of global bifurcation behaviour will be considered. In particular we shall consider the degeneration of the Hopf ellips into some sort of attractor and the interesting phenomenon of a Feigenbaum scenario in the case of strong resonance 1 : 4.

2. A LOGISTIC DELAY MAP

The difference equation

$$x_{n+1} = ax_n(1-(1-b)x_n-bx_{n-1}) \tag{2.1}$$

belongs to a wide class of models in population dynamics describing the number of individuals in successive generations. In this interpretation we have $0 \leq x_n \leq 1$, $a > 0$ and $0 \leq b \leq 1$. The cases $b = 0$ and $b = 1$ are well known and some of the properties of the simpler models are also valid in this more general case.

There are the two equilibrium states $x = 0$ and $x = 1 - 1/a$. They correspond to fixed points in the equivalent planar map

$$\begin{cases} x' = y \\ y' = ay(1-bx-(1-b)y). \end{cases} \tag{2.2}$$

The origin is stable up to a = 1. The multipliers of the other fixed point are the roots of

$$\lambda^2 - \lambda(2-a-b+ab) + b(a-1) = 0. \tag{2.3}$$

A simple calculation shows that the stability region in the a,b-plane is determined by a > 1 and

$$a < \frac{3-2b}{1-2b} \quad \text{for } b \leqq 1/4, \tag{2.4}$$

and

$$a < 1 + \frac{1}{b} \quad \text{for } b \geqq 1/4. \tag{2.5}$$

The stability region in the parameter plane a,b is sketched in fig. 2.1.

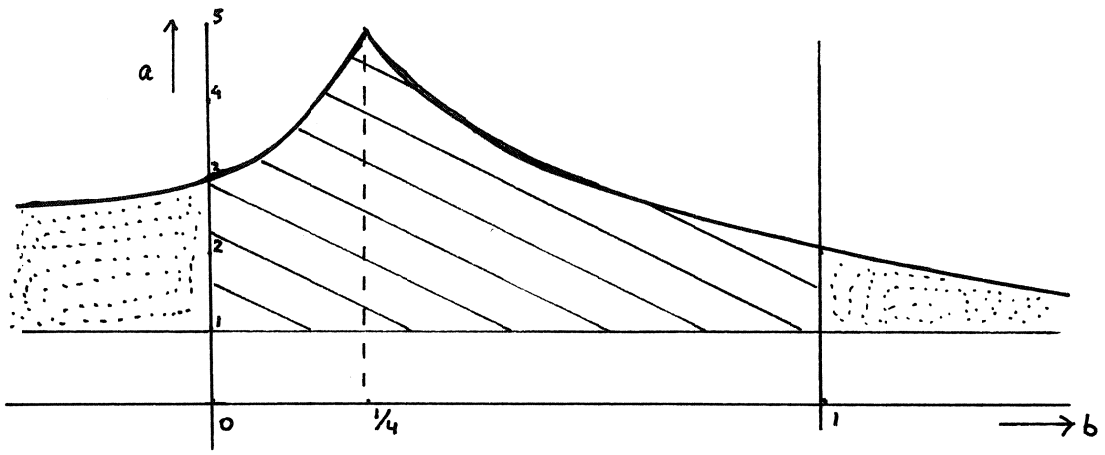

Fig. 2.1.

At the boundary a = 1 the two fixed points (0,0) and (1-1/a, 1-1/a) are coalescing. The multipliers are $\lambda = 0$ and $\lambda = 1$. At the boundary (2.4) we have a multipier -1. At the boundary (2.5) we have a pair of complex roots on the unit circle $\lambda = \exp i\alpha$ and $\bar{\lambda} = \exp(-i\alpha)$. The critical values

of a and b are

$$(2.6)\qquad \begin{cases} a = 3 - 2\cos\alpha, \\ b = \dfrac{1}{2(1-\cos\alpha)}. \end{cases}$$

If b is restricted to the interval (1/4,1) the possible values of α are in the interval $(\pi/3,\pi)$. We list a few special cases

a	b	α	
2	1	$\pi/3$	weak resonance 1 : 6
2.3820	0.7236	$2\pi/5$	" " 1 : 5
3	0.5	$\pi/2$	strong " 1 : 4
4	1/3	$2\pi/3$	" " 1 : 3

Local bifurcation at the latter boundary can be studied by taking

$$(2.7)\qquad \lambda = (1+\mu)e^{i\alpha}.$$

The corresponding values of a and b can be calculated from

$$(2.8)\qquad \begin{cases} a = 2 - (\lambda+\bar{\lambda}) + \lambda\bar{\lambda}, \\ b = \lambda\bar{\lambda}/(a-1). \end{cases}$$

This gives

$$(2.9)\qquad a = (3-2\cos\alpha) + 2\mu(1-\cos\alpha) + \mu^2,$$

and

$$(2.10)\qquad (a-1)b = 1 + 2\mu + \mu^2.$$

However, in the case of a p/q-resonance when

(2.11) $\alpha = 2\pi p/q$

it is better to describe the local bifurcation by

(2.12) $\lambda = e^{i\alpha}(1+\mu e^{i\phi})$.

The parameters μ and ϕ can be considered as polar coordinates in a small neighbourhood of the critical value $\lambda = \exp i\alpha$ as shown in fig. 12

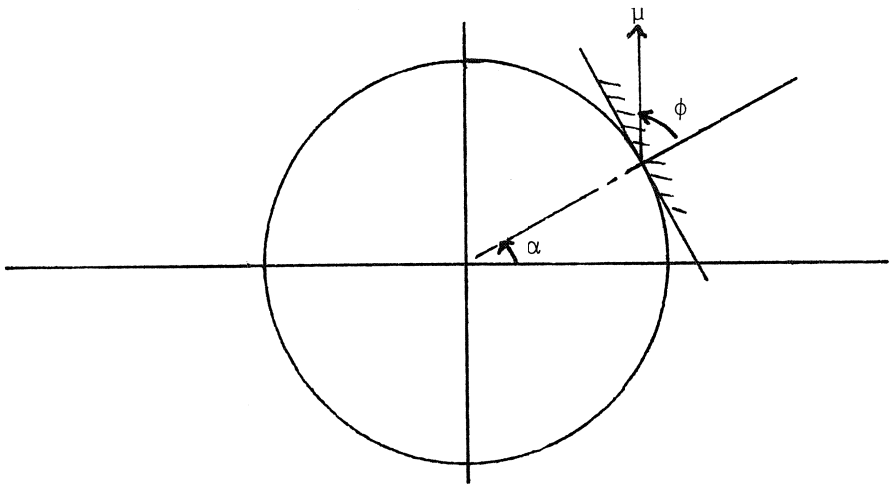

Fig. 2.1.

-

The map (2.2) can be written in the form (1.3) by taking the fixed point $(1-1/a, 1-1/a)$ as the new origin of a translated coordinate system. We obtain at once

(2.13) $$\begin{cases} x' = y, \\ y' = Ax + By - abxy - a(1-b)y^2, \end{cases}$$

with

(2.14) $A = -\lambda\bar{\lambda}, \quad B = \lambda + \bar{\lambda}.$

In Appendix C an expression is derived for the Hopf ellipse excluding the cases of strong resonance. The result is

$$x^2 - 2xy \cos\alpha + y^2 = R^2 \tag{2.15}$$

with

$$R^2 = \frac{32\mu \sin^4 \alpha}{3a^2}, \tag{2.16}$$

of course with $a = 3 - 2 \cos\alpha$.
The semi-axes of this Hopf ellipse are

$$\frac{R}{\sqrt{2}\sin\alpha/2}, \quad \frac{R}{\sqrt{2}\cos\alpha/2}. \tag{2.17}$$

An elementary calculation shows that with respect to α the Hopf radius is a maximum for $\cos\alpha = (3-\sqrt{5})/2$ corresponding to ab. 68°. The area of the Hopf ellipse is maximal for $\alpha = 60^\circ$. The following table gives an idea of what can be expected for various values of α (in degrees)

α	a	b	$R/\sqrt{\mu}$	$\tan \alpha/2$
20	1.121	8.291	0.341	0.176
30	1.268	3.732	0.644	0.268
36	1.382	2.618	0.816	0.325
40	1.468	2.137	0.919	0.364
45	1.586	1.707	1.030	0.414
60	2	1	1.225	0.577
72	2.382	0.724	1.240	0.727
80	2.653	0.605	1.194	0.839
90	3	$\frac{1}{2}$	1.089	1
108	3.618	0.382	0.816	1.376
120	4	1/3	0.612	1.732
135	4.414	0.293	0.370	2.414
144	4.618	0.276	0.244	3.078

In order to determine the position of the Arnold horn ϕ at the point $\exp i\alpha$ of weak resonance $\alpha = 2\pi p/q$ we have to determine $\gamma = \arg Q$ where Q is the essential parameter of the corresponding normal form

$$w = \lambda z - Qz^2\bar{z} + \ldots \tag{2.18}$$

where $\lambda = (1+\mu)\exp i\alpha$.

The axis of the Arnold horn then is $\phi = \gamma - \alpha$. In Appendix C it is shown how Q can be obtained for the more general map (1.3) via the pre-normal map

$$w = \lambda z + (a_{20}z^2 + a_{11}z\bar{z} + a_{02}\bar{z}^2) \tag{2.19}$$

with

$$z = ix\bar{\lambda} - iy. \tag{2.20}$$

A simple calculation shows that

$$\begin{cases} 4ia_{20}\sin^2\alpha = \dfrac{\lambda^3}{1-\lambda}\, a, \\ 4ia_{11}\sin^2\alpha = -a, \\ 4ia_{02}\sin^2\alpha = \dfrac{\bar{\lambda}^3}{1-\bar{\lambda}}\, a, \end{cases} \tag{2.21}$$

of course with $a = 3 - 2\cos\alpha$.

Eventually we obtain using the results of Appendix C

$$\gamma - \alpha = \arg(e^{-i\alpha}Q) = \arg((1+\cos\alpha)+i(3\sin\alpha+\cot\tfrac{3}{2}\alpha)). \tag{2.22}$$

The following table gives the values of the right-hand side of (2.22) for a few values of α. We note that $\alpha = 120^\circ$ is exceptional being a case of strong resonance. Further $\gamma - \alpha$ changes considerably in the interval (100, 110).

α^o	$\gamma^o-\alpha^o$		α^o	$\gamma^o-\alpha^o$
0	90		90	63
10	65		100	56
20	55		110	-54
30	53		120	--
40	55		130	87
50	57		140	86
60	60		150	87
70	62		160	88
80	64		170	89

In particular for a few cases at low resonance we have

p : q	α^o	a	b	$R/\sqrt{\mu}$	$\gamma^o-\alpha^o$
1 : 6	60	2	1	1.225	60
1 : 5	72	2.382	0.724	1.240	62.6
2 : 9	80	2.653	0.605	1.194	63.7
3 : 10	108	3.618	0.382	0.816	-18.0
3 : 8	135	4.414	0.293	0.370	86.3
2 : 5	144	4.618	0.276	0.244	86.5

2. CREMONA TRANSFORMATION

For a full understanding of the properties of the mapping (1.1) it may be helpful to consider (1.1) as a Cremona transformation of the second order in the projective plane. By this we understand an invertible mapping of the form

$$(3.1) \qquad x' : y' : z' = \phi(x,y,z) : \psi(x,y,z) : \chi(x,y,z)$$

where x,y,z are projective coordinates in a plane Π and x',y',z' similar coordinates in a plane Π'. The two planes may be different or not. The functions ϕ,ψ,χ are homogeneous quadratic polynomials. The inverse of (1.1) is of the same form.

By (3.1) lines in the Π'-plane are transformed into conics in the Π-plane. In the general case all those conics pass through three special points A,B,C so-called fundamental points, forming the fundamental triangle in Π. Similarly there is a fundamental triangle A'B'C' in Π' with the property that all conics through A'B'C' correspond to lines in Π. The Cremona transformation is 1 - 1 except for the fundamental triangles. The main properties of this mapping are described in the following table

Π	Π'
line	conic through A'B'C'
point of AB	C'
line through A	line through A' (+ B'C')
conic through A,B,C	line (+ sides of A'B'C')
conic through A,B	conic through A',B' (+ two sides)
conic through A	cubic curve (+ B'C')

These properties mean for (3.1) that the polynomials ϕ,ψ and χ vanish simultaneously for three different points, at least different in the general case. Of course there are quite a number of special cases where two or more fundamental points coincide. We shall soon see that our map (1.1) is a rather degenerate case.

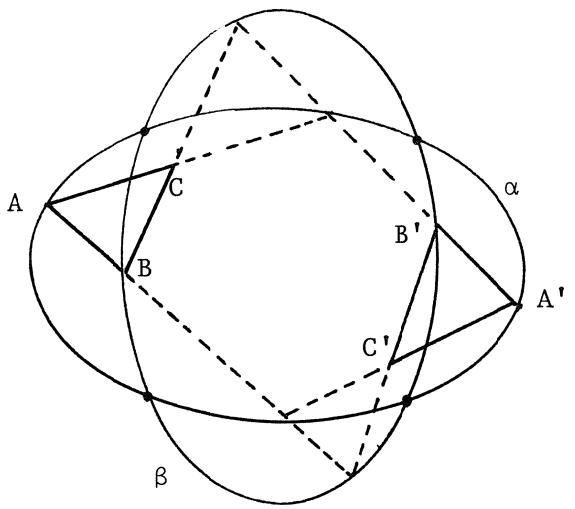

Fig. 3.1.
A general Cremona transformation

When the two planes Π and Π' are identified we have the further possibility of fixed points. We also have the following nice geometrical interpretation. Let P and P' be corresponding points then the pencils AP and A'P' are in a projective correspondence. This means that the intersections of AP and A'P' are situated on a certain conic α passing through A and A'. In a similar way we have other conics β through B,B' and γ through C,C'. Any fixed point of the Cremona map should be a common point of α,β,γ. This shows that there are four fixed points, cf. fig. 3.1.

For the map (1.1) we have

$$(3.2) \qquad x' : y' : z' = yz : ay(z-bx-(1-b)y) : z^2$$

in the projective notation of (3.1). The inverse map is

$$(3.3) \qquad x : y : z = ax'z' - a(1-b)x'^2 - y'z' : abx'^2 : abx'z'.$$

The fundamental triangles are A,B (1,0,0) coinciding along y = 0 with C(1-b,-b,0) and A',B'(0,1,0) coinciding along z = 0 with C'(0,0,1), cf. fig. 3.2.

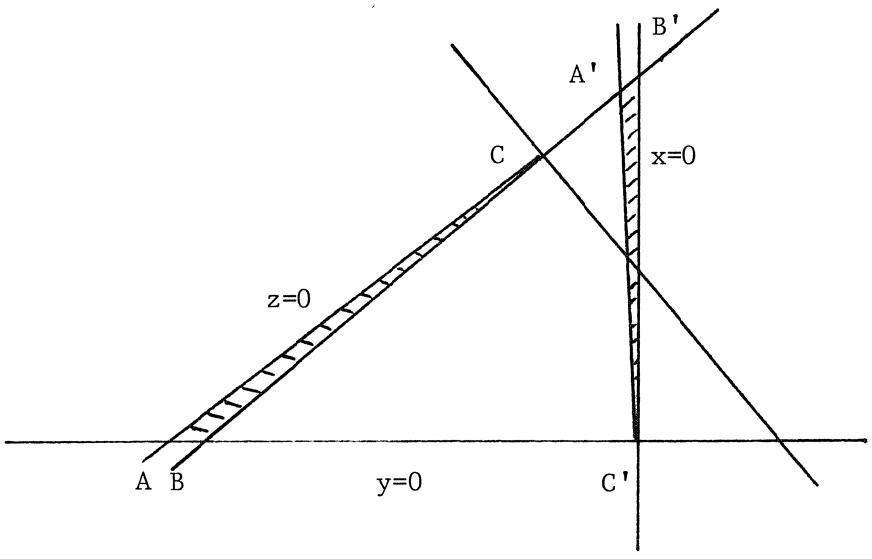

Fig. 3.2. The logistic delay map as a special Cremona transformation

The four fixed points are $C'(0,0,1)$, $F(1-1/a,1-1/a,1)$ and the two infinite points $C(1-b,-b,0)$, $A'(0,1,0)$.

However, since C is a fundamental point of Π it is a fixed point only for the inverse map (3.3), for the direct map (3.2) it is a singularity and has no meaning. On the other hand C' and A' are true fixed points of the direct map (3.2) but for the inverse map (3.3) they have no meaning. The conics α and β are degenerated into a pair of lines. The conic α becomes the line at infinity $z = 0$ and the line C'F, β is the same pair. The conic γ is in Cartesian coordinates (x for x/z, y for y/z) the hyperbole

$$x = ay(1-bx-(1-b)y). \tag{3.4}$$

The nature of the fixed points C' and F is well known. In order to study the local behaviour of the fixed point $A'(0,1,0)$ we consider x/y and z/y as Cartesian coordinates with $y = 0$ being the infinite line. Then (3.2) is equivalent to the metric map

$$\begin{cases} x' = \dfrac{z}{a(z-bx-1+b)}, \\ z' = \dfrac{z^2}{a(z-bx-1+b)}. \end{cases} \tag{3.5}$$

The local behaviour is determined by

$$x' \approx \frac{z}{a(-1+b)}, \quad z' \approx \frac{z^2}{a(-1+b)}. \tag{3.6}$$

This shows that for $b \neq 1$ the fixed point A' is always locally attracting.

For the original map (1.1) this means that points escape into infinity asymptotically along a parabolic branch

$$y = -a(1-b)x^2. \tag{3.7}$$

The nature of the fixed point C of the inverse map is even more interesting. If we take the inverse of (3.5) we obtain the map

$$(3.8)\qquad \begin{cases} x = \dfrac{(a-1)z'}{abx'} - \dfrac{1-b}{b}, \\ z = z'/x', \end{cases}$$

for which C is a fixed point with $x = -(1-b)/b$, $z = 0$. Its multipliers are 0 and $-b/(1-b)$. Thus C is repelling for $b > \frac{1}{2}$ and attracting for $b < \frac{1}{2}$. The important special $b = \frac{1}{2}$ case requires a more detailed analysis. Consider the original difference equation

$$(3.9)\qquad x_{n+1} = ax_n(1-\tfrac{1}{2}x_n-\tfrac{1}{2}x_{n-1}).$$

Its inverse can be written as

$$(3.10)\qquad u_{n+1} = 2 - u_n - \frac{2u_{n-1}}{au_n}.$$

To this we may apply a perturbation technique in order to solve (3.10) in an asymptotic way.
Eventually we obtain the result

$$(3.11)\qquad u_n \approx (-1)^n\, c\sqrt{n} + O(1)$$

with

$$(3.12)\qquad c = \frac{2}{a}\sqrt{2a+2}.$$

For the inverse map this means that an orbit may go to infinity in a very slow way. The fixed point C(-1,1,0) is still locally attracting but in a rather marginal way.

The maps (3.2), (3.3) can be replaced by projectively equivalent maps in a number of ways. Here we give a single example.

$$(3.13)\qquad \begin{cases} x' = \dfrac{-qy(y-q)}{m(y-q)^2+y(x-p)}, \\ y' = \dfrac{qy(x-p)}{m(y-q)^2+y(x-p)}. \end{cases}$$

The inverse looks a bit simpler

$$(3.14)\qquad \begin{cases} x = p + \dfrac{qy'(y'-q)}{x'(mx'-y'+q)}, \\ y = \dfrac{mqx'}{mx'-y'+q}. \end{cases}$$

The four fixed points are all on the circle $x^2 + y^2 - px - qy = 0$. They are, in the same notation as before (cf. fig. 3.3)

$$C'(0,0),\quad A'(0,q),\quad C(p,q),\quad F\left(\frac{p+qm}{1+m^2},\ \frac{m(p+qm)}{1+m^2}\right).$$

Again this is a two-parameter map with p/q and m as independent parameters. A map like (3.13) is a convenient object to study since there is no "trouble at infinity".

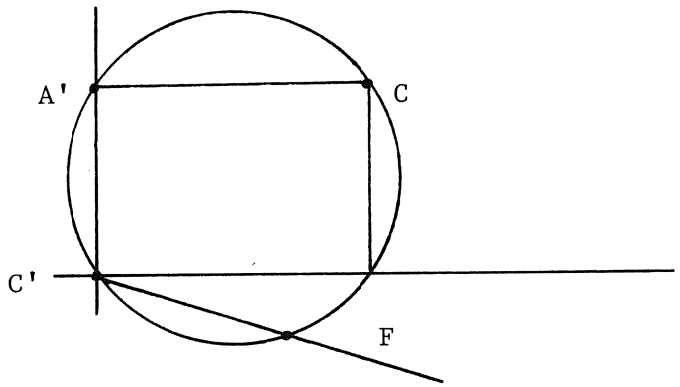

Fig. 3.3. A projectively equivalent version of the logistic delay map

4. ILLUSTRATIONS

The illustrations given here illustrate the various points of the theory. In all cases the map (1.1) in the form (2.13) has been used with the unstable fixed point at the centre of the picture.

Fig. 4.1 $\alpha = 2\pi/6$, $\mu = 0.005$, $\phi = 0$.
Scale -0.2, 0.2, -1.33, 1.33.

Illustration of Hopf bifurcation in the case of weak resonance 1 : 6. The Hopf ellipse is of maximum area. The semi-axes are in first-order approximation $\sqrt{3\mu} = 0.1225$ and $\sqrt{\mu} = 0.0707$. All points belong to a single orbit.

Fig. 4.2 $\alpha = 1.1789$, $\mu = 0.005$, $\phi = 0$.
Scale -0.2, 0.2, -1.33, 1.33.

Illustration of Hopf bifurcation in the irrational case $\alpha = \arccos\frac{1}{2}(3-\sqrt{5})$ where the radius of the Hopf circle is maximal. In degrees $\alpha = 67^{\circ}.5445 \approx 67^{\circ}.5 = \frac{3}{16}.360^{\circ}$ so that we are close to resonance 3 : 16.

Fig. 4.3 $\alpha = 1.1789$, $\mu = 0.02$, $\phi = \pi/3$.
Scale -0.6, 0.6, -0.4, 0.4.

A similar case as before but taken close to the axis of the Arnold horn of the weak resonance 3 : 16. A single orbit is shown which seems to converge to a stable 16-cycle.

Fig. 4.4 $\alpha = 2\pi/5$, $\mu = 0.02$, $\phi = \pi/3$.
Scale -0.6, 0.6, -0.4, 0.4.

The case of the lowest weak resonance taken close to the axis of the Arnold horn. Two orbits are shown perhaps converging to a stable 5-cycle as predicted in the theory.

Fig. 4.5 $\alpha = \pi/2$, $\mu = 0.01$, $\phi = -\pi/3$.
Scale -0.3, 0.3, -0.2, 0.2.

Illustration of a deformed Hopf ellipse, a rounded square, in this case of strong resonance. The theory for this case has been given in [3].

Fig. 4.6 $\alpha = 3\pi/5$, $\mu = 0.01$, $\phi = \pi/6$.
Scale -0.6, 0.6, -0.4, 0.4.

Illustration of bifurcation at resonance 3 : 10 which is close to the strong 1 : 3 resonance. This explains the rounded triangular pattern.

Fig. 4.7 $\alpha = \pi/\sqrt{2}$, $\mu = 0.002$, $\phi = 0$.
Scale -0.2, 0.2, -0.133, 0.133.

Illustration of Hopf bifurcation in the irrational case $1 : \sqrt{8} = 1 : 2.8284 \approx 1 : 2.8333 = 6 : 17$. In degrees $\alpha = 127^{o}.0588 \approx 127^{o}.2792$. The triangular pattern is due to the claseness of the strong 1 : 3 resonance with $\alpha = 120^{o}$.

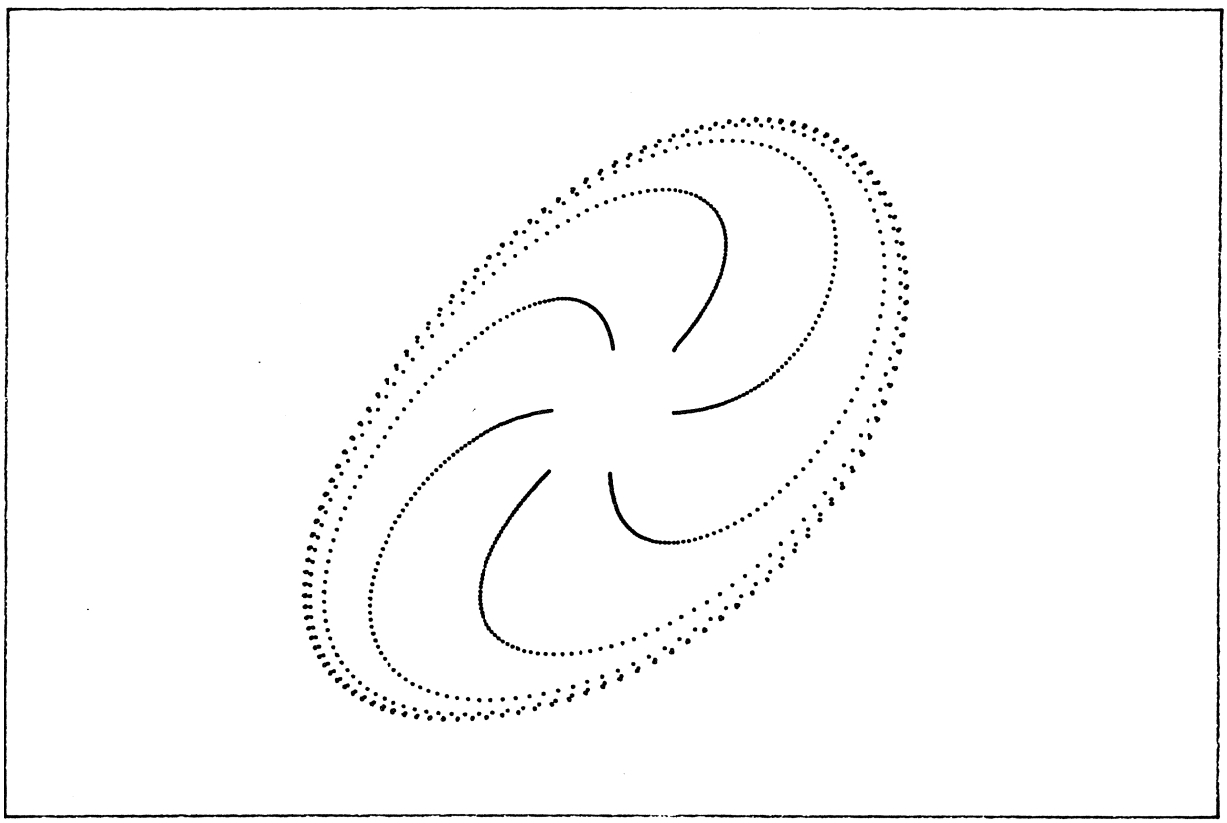

Fig. 4.1.

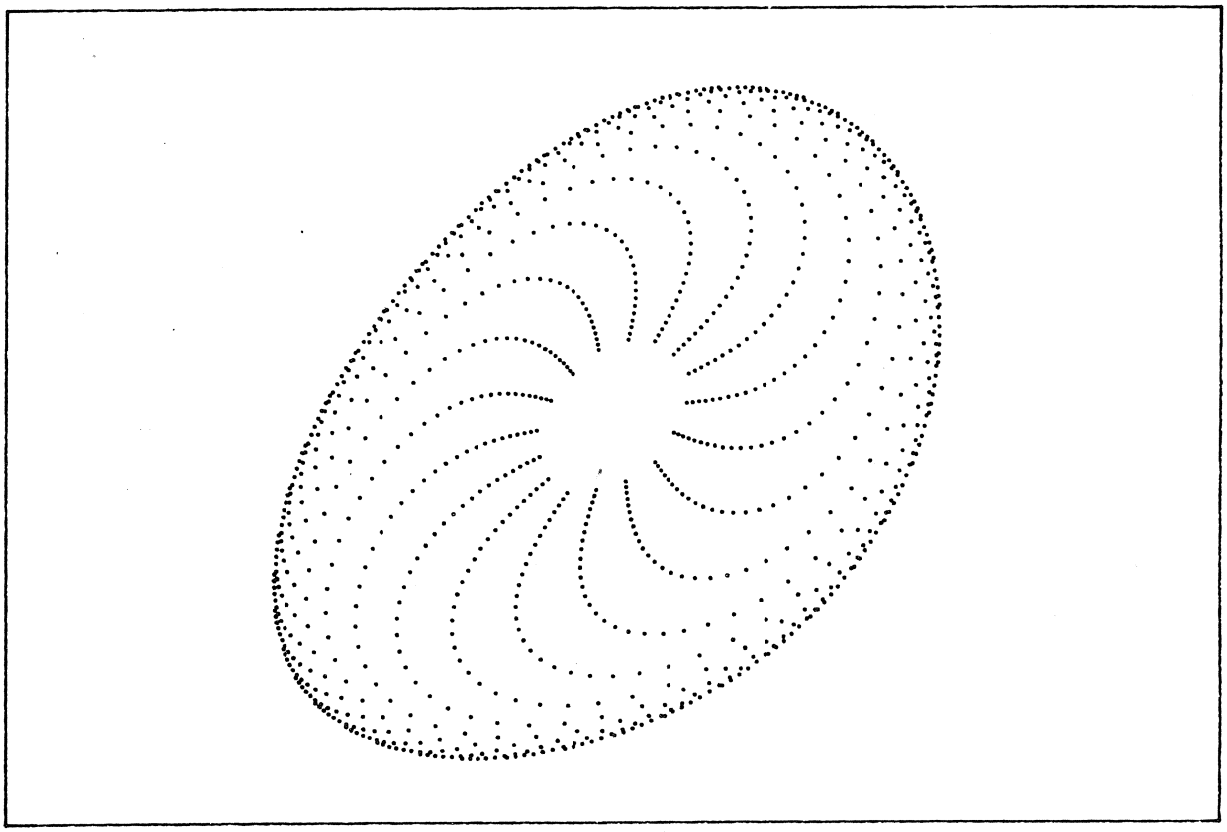

Fig. 4.2.

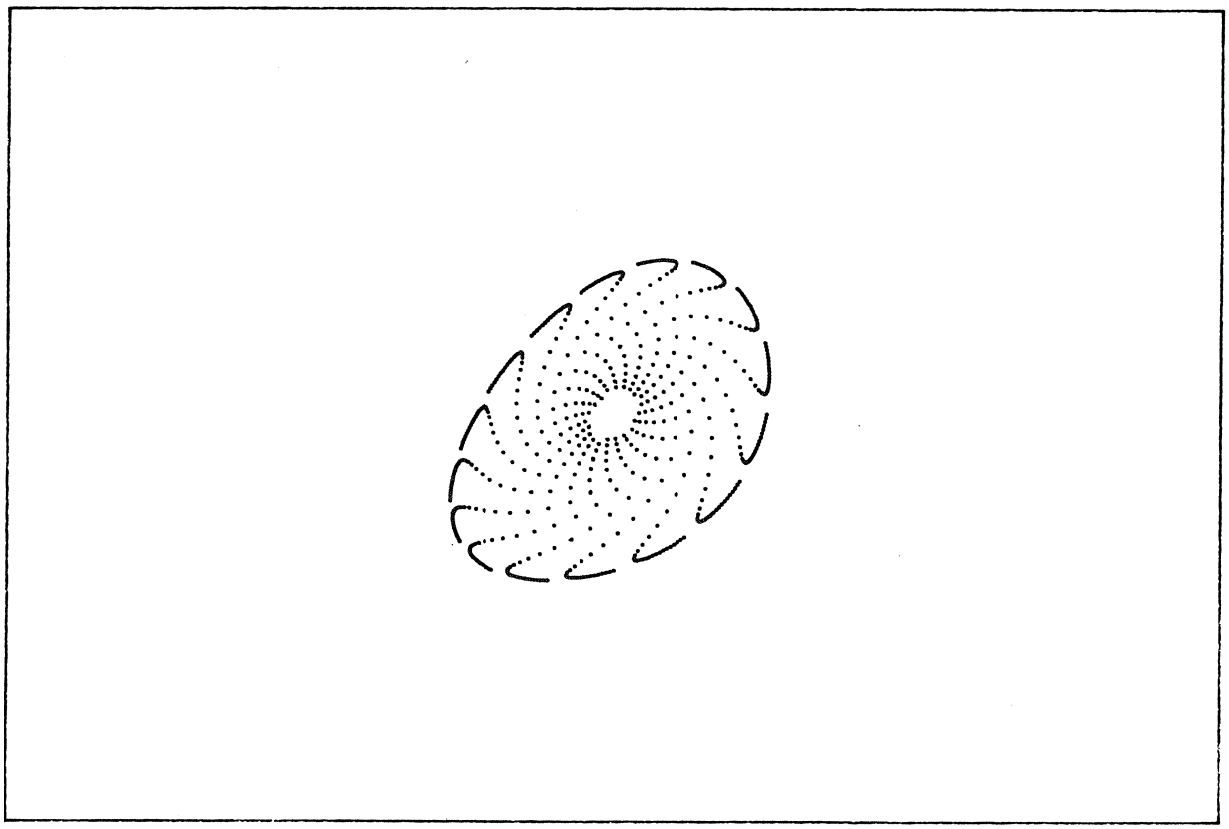

Fig. 4.3.

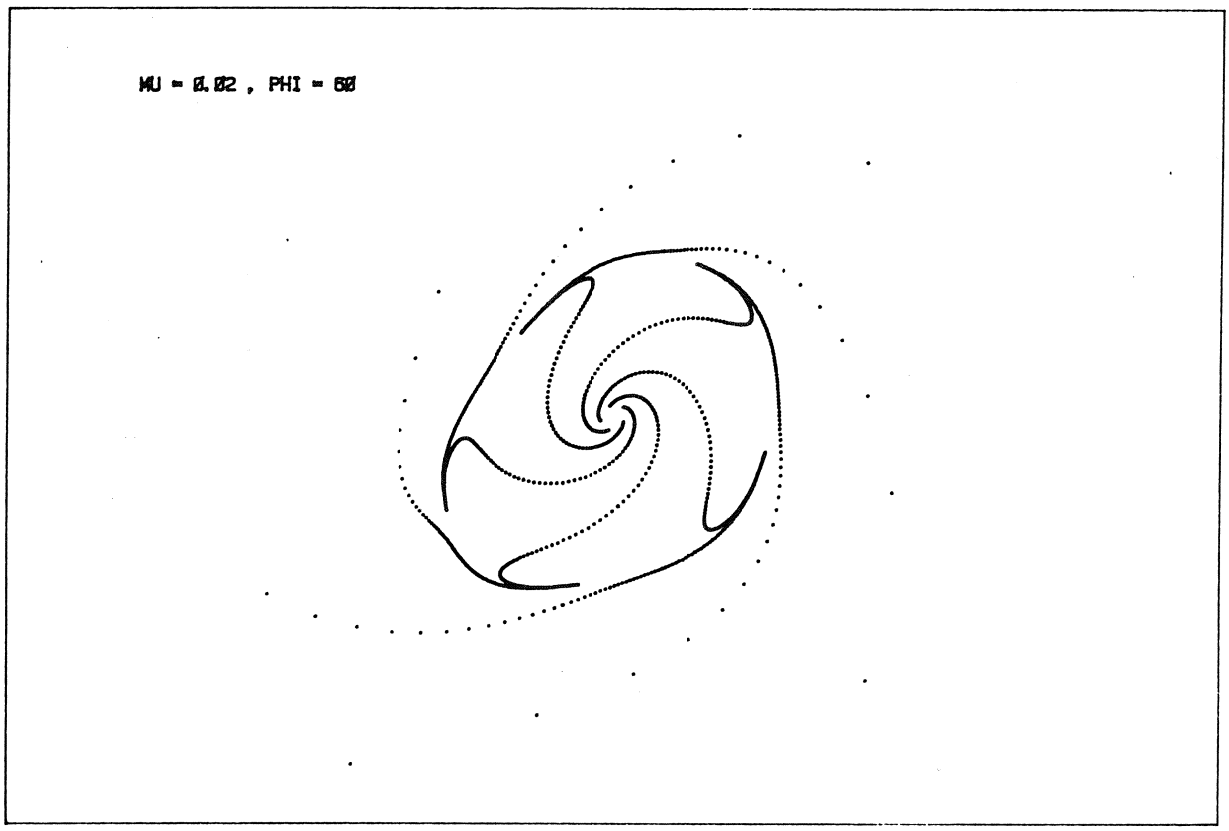

Fig. 4.4.

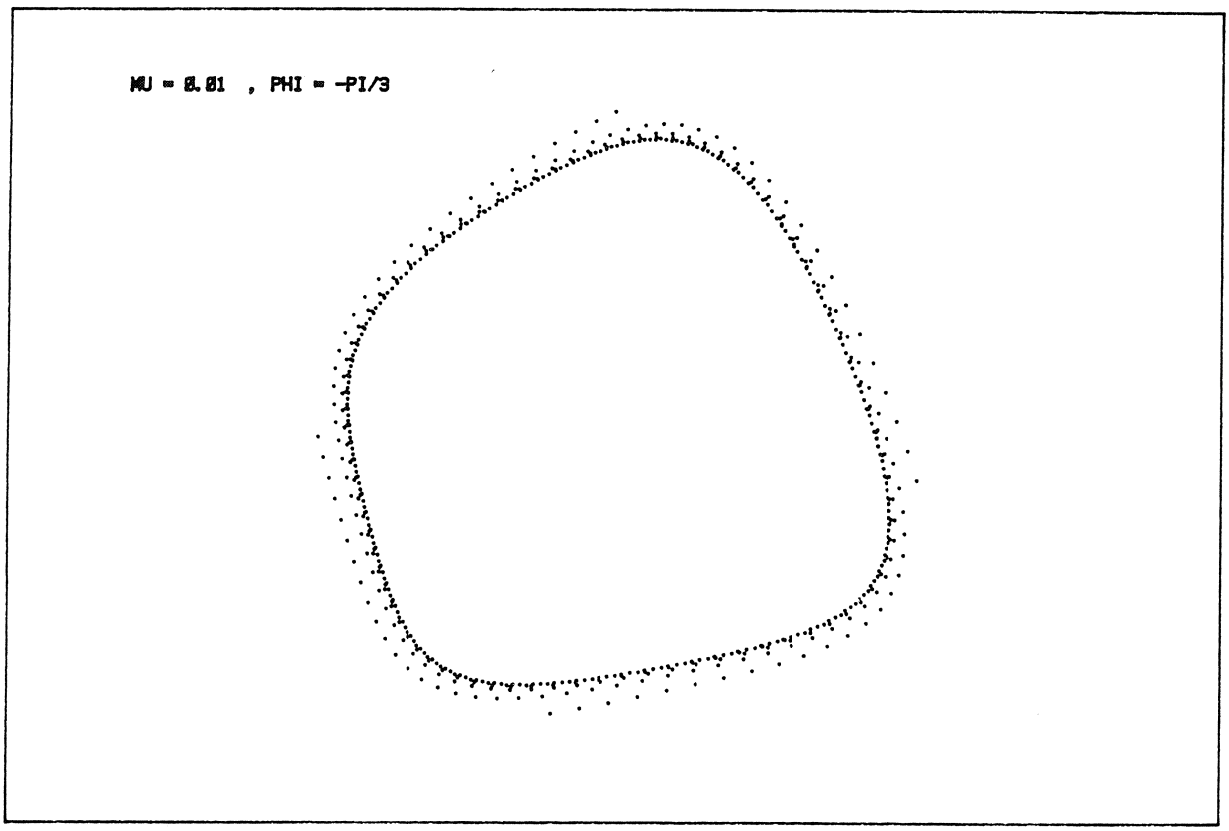

Fig. 4.5.

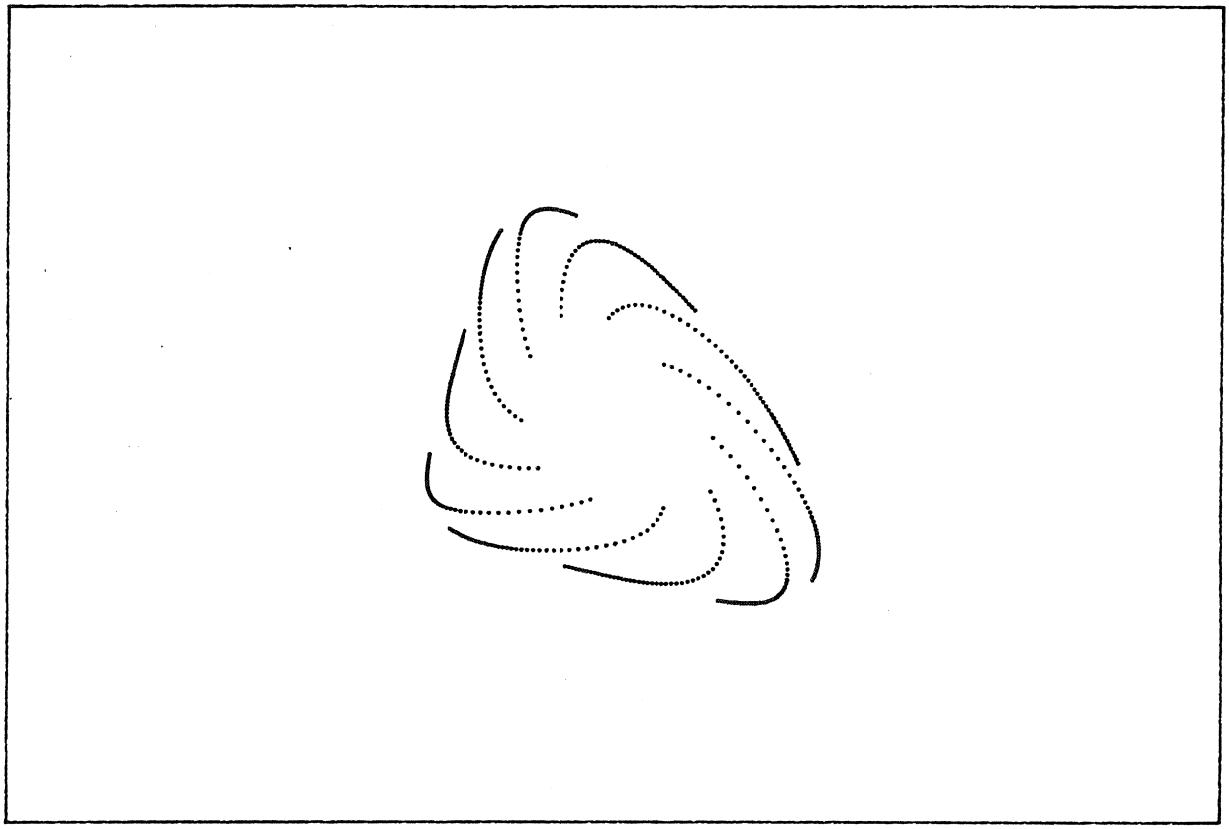

Fig. 4.6.

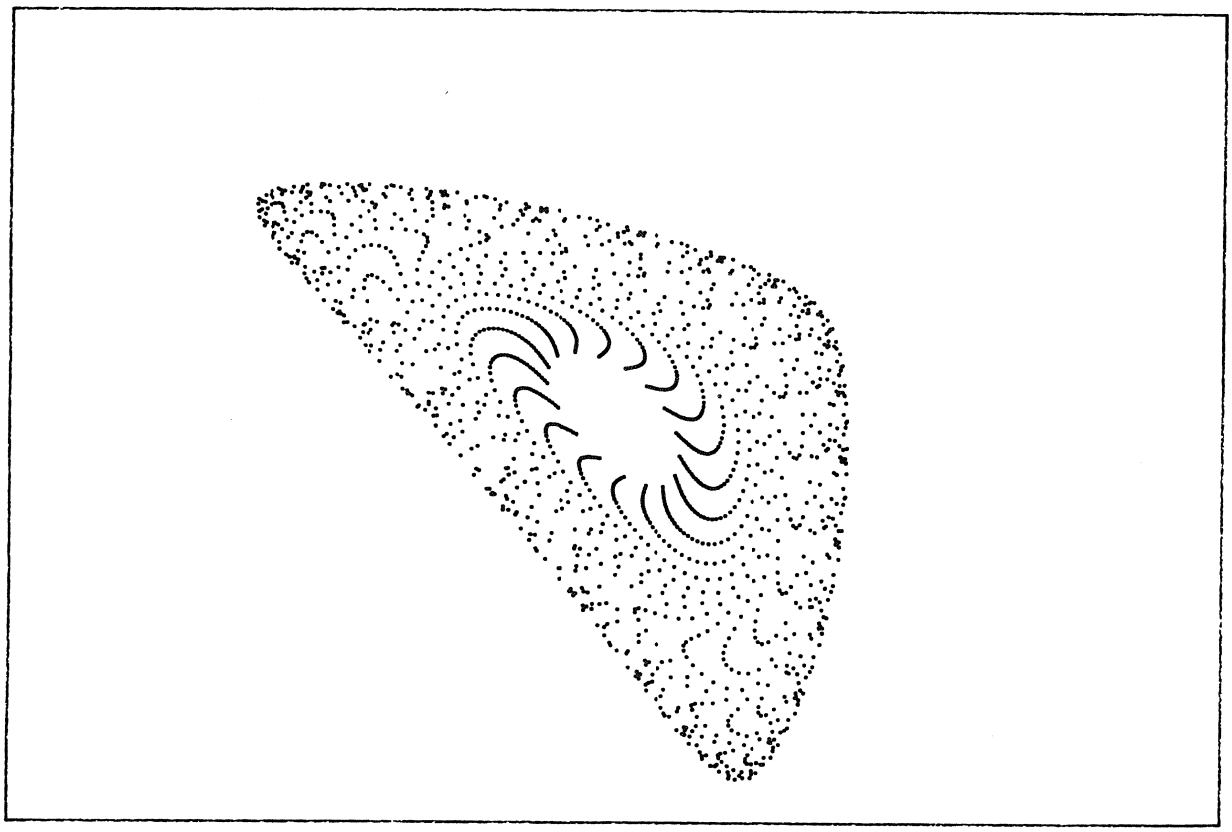

Fig. 4.7.

Appendix A

We consider the complex analytic map

$$w = \lambda z + A_2(z,\bar{z}) + A_3(z,\bar{z}) + \ldots \tag{A1}$$

where the origin is a fixed point of marginal stability

$$\lambda = e^{i\alpha} + O(\mu) \tag{A2}$$

and where $A_j(z,\bar{z})$ is a homogeneous polynomial of degree j in $z = x + iy$ and $\bar{z} = x - iy$. Explicitly we write

$$\begin{cases} A_2(z,\bar{z}) = a_{20}z^2 + a_{11}z\bar{z} + a_{02}\bar{z}^2 \\ A_3(z,\bar{z}) = a_{30}z^3 + a_{21}z^2\bar{z} + a_{12}z\bar{z}^2 + a_{03}\bar{z}^3 \end{cases} \tag{A3}$$

etcetera.

It is well known that by a suitable transformation of coordinates the map (A2) can be written in a much simpler form provided certain resonances are excluded.

In particular if $\lambda^3 \neq 1$ and $\lambda^4 \neq 1$ it is always possible to remove the quadratic term and part of the cubic term. Then (A1) can be reduced to the so-called normal form

$$w = \lambda z - Qz^2\bar{z} + \ldots . \tag{A4}$$

More generally if α/π is rational and if q is the lowest positive integer such that

$$\alpha = 2\pi p/q, \quad q \geq 4, \tag{A5}$$

then (A1) can be reduced to the normal form

$$\begin{aligned} w = \lambda z + c_1 z^2\bar{z} + c_2 z^3\bar{z}^2 + \ldots + c_{q/2-1} z^{q/2}\bar{z}^{q/2-1} + \\ + c_{q/2}\bar{z}^{q-1} + O(z^{q+1}) \end{aligned} \tag{A6}$$

for even q, and

$$w = \lambda z + c_1 z^2\bar{z} + c_2 z^3\bar{z}^2 + \ldots + c_{(q-3)/2} z^{(q-1)/2}\bar{z}^{(q-3)/2} + \tag{A7}$$
$$+ c_{(q-1)/2}\bar{z}^{q-1} + O(z^q)$$

for odd q.

The proof of these statements is a matter of book-keeping. Let us consider the normal form (A4) as the result of the coordinate transformation

$$\begin{cases} z_0 = z + P_2(z,\bar{z}) + P_3(z,\bar{z}) + \ldots \\ w_0 = w + P_2(w,\bar{w}) + P_3(w,\bar{w}) + \ldots \end{cases} \tag{A8}$$

where $P_k(z,\bar{z}) = \Sigma_{i+j=k}\, p_{ij} z^i \bar{z}^j$.

If this is applied to (A1) the result will be (A4) written in new coordinates z_0 and w_0.
Substitution of (A8) gives in old coordinates

$$\begin{aligned} & w + P_2(w,\bar{w}) + P_3(w,\bar{w}) + \ldots = \\ & = \lambda(z+P_2(z,\bar{z})+P_3(z,\bar{z})+\ldots) - \\ & - Q(z+\ldots)^2(\bar{z}+\ldots) + \ldots . \end{aligned} \tag{A9}$$

Substitution of (A1) on the left-hand side turns this into an identity. Taking only terms up to the third order we find

$$\begin{aligned} & \lambda z + A_2(z,\bar{z}) + A_3(z,\bar{z}) + p_{20}(\lambda^2 z^2 + 2\lambda z\, A_2(z,\bar{z})) + \\ & + p_{11}(\lambda\bar{\lambda}z\bar{z} + \lambda z\bar{A}_2(\bar{z},z) + \bar{\lambda}\bar{z}A_2(z,\bar{z})) + \\ & + p_{02}(\bar{\lambda}^2\bar{z}^2 + 2\bar{\lambda}\bar{z}\bar{A}_2(\bar{z},z)) + P_3(\lambda z,\bar{\lambda}\bar{z}) \equiv \\ & \equiv \lambda z + \lambda P_2(z,\bar{z}) + \lambda P_3(z,\bar{z}) - Qz^2\bar{z}. \end{aligned} \tag{A10}$$

Equating equal coefficients of z^2, $z\bar{z}$ and $\bar{z}^2$ we obtain

$$\text{(A11)}\qquad \begin{cases} a_{20} + \lambda^2 p_{20} = \lambda p_{20}, \\ a_{11} + \lambda\bar{\lambda} p_{11} = \lambda p_{11}, \\ a_{02} + \bar{\lambda}^2 p_{02} = \lambda p_{02}. \end{cases}$$

Since we have excluded the lower resonances $\lambda^3 = 1$ it is possible to find coefficients p_{20}, p_{11}, p_{02} which guarantee the vanishing of the quadratic part $A_2(z,\bar{z})$. A similar computation carried out for the term $z^j\bar{z}^k$ would require the condition

$$\lambda^{j-k} \neq \lambda.$$

Thus all such terms can be removed by the same trick with the exception of $j = k+1$ i.e. $z^2\bar{z}$, $z^3\bar{z}^2$,... etcetera.

In the case of the resonance (A5) we have the further exception $j = 0$, $k = q-1$ which gives the term $\bar{z}^{q-1}$.

Next we shall derive a useful expression for Q which can be used for the discussion of actual maps. Since we are interested only in the lowest order approximation with respect to μ we need the coefficients a_{20}, p_{20} ... only for $\mu = 0$.

From (A11) we obtain

$$\text{(A12)}\qquad p_{20} = \frac{a_{20}}{\lambda-\lambda^2}, \quad p_{11} = \frac{a_{11}}{\lambda-1}, \quad p_{02} = \frac{a_{02}}{\lambda-\bar{\lambda}^2},$$

where $\lambda = \exp i\alpha$.

From (A10) we obtain

$$\text{(A13)}\qquad -Q = a_{21} + 2\lambda a_{11}p_{20} + (\lambda\bar{a}_{11}+\bar{\lambda}a_{20})p_{11} + 2\bar{\lambda}\bar{a}_{02}\bar{p}_{02}.$$

Substitution of the coefficients (A12) gives

$$\text{(A14)}\qquad -Q = a_{21} + \frac{|a_{11}|^2}{1-\bar{\lambda}} + \frac{2|a_{02}|^2}{\lambda^2-\bar{\lambda}} + \frac{2\lambda-1}{\lambda(1-\lambda)}\, a_{11}a_{20}.$$

Appendix B

Hopf bifurcation and Arnold horn

Excluding the cases of strong resonance we may have Hopf bifurcation. The appropriate normal form is

$$w = \lambda z - Qz^2\bar{z} + O(z^4) \tag{B1}$$

where

$$\lambda = (1+\mu)e^{i\alpha} \tag{B2}$$

and Q is taken at $\mu = 0$.
From (B1) we obtain

$$|w|^2 = |z|^2 \left(|\lambda|^2 - (\lambda\bar{Q}+\bar{\lambda}Q)|z|^2 + \ldots\right). \tag{B3}$$

If R is the radius of an invariant circle we should have

$$1 = 1 + 2\mu - (\lambda\bar{Q}+\bar{\lambda}Q)R^2 + \ldots . \tag{B4}$$

Writing

$$Q = ce^{i\gamma} \tag{B5}$$

we find at once

$$R^2 = \frac{\mu}{c\cos(\alpha-\gamma)} + O(\mu^2). \tag{B6}$$

The explicit expression (A14) can be used to obtain a similar expression for the Hopf radius. Starting from

$$\frac{\mu}{R^2} = \mathrm{Re}(\bar{\lambda}Q) \tag{B7}$$

we obtain at once

$$\text{(B8)}\qquad \frac{\mu}{R^2} = \tfrac{1}{2}|a_{11}|^2 + |a_{02}|^2 - \mathrm{Re}\,\frac{(2-\bar{\lambda})a_{11}a_{20}}{\lambda(1-\lambda)} - \mathrm{Re}\bar{\lambda}a_{21}.$$

(B6) shows that the possibility of a real Hopf circle depends on the sign of $\cos(\alpha-\gamma)$.

Next we consider the phenomenon of a so-called Arnold horn close to resonance $\alpha = 2\pi p/q$. Instead of (B1) we take

$$\text{(B9)}\qquad \lambda = (1+\mu e^{i\phi})e^{i\alpha}.$$

This means that μ and ϕ can be considered as local polar coordinates at the resonance point $\exp 2\pi pi/q$ in the complex λ-plane.

Arnold's result can easily be obtained from the normal forms (A6) and (A7). Assuming that existence of a real Hopf radius R we may write the normal form as

$$\text{(B10)}\qquad w = z(\lambda+c_1R^2+c_2R^4+\ldots) + C\bar{z}^{q-1} + \ldots .$$

Taking arguments with $\theta = \arg z$ and $\theta' = \arg w$ we obtain

$$\text{(B11)}\qquad \theta' = \theta + \alpha + \arg((1+\mu e^{i\phi}) - Qe^{-i\alpha}R^2 + \ldots + CR^{q-2}e^{-iq\theta}) + \ldots .$$

Using the first order expressions

$$\text{(B12)}\qquad \begin{cases} Q = c\ \exp i\gamma, \\ R^2 = \dfrac{\mu\cos\phi}{c\cos(\alpha-\gamma)}, \end{cases}$$

we find

$$\text{(B13)}\qquad \theta' = \theta + \alpha + \arg(1+i\mu\frac{\sin(\phi+\alpha-\gamma)}{\cos(\alpha-\gamma)} + \ldots + C\mu^{\frac{q-2}{2}}e^{-iq\theta}).$$

The existence of a periodic q-cycle implies the existence of a θ-value such that in a first order approximation

$$\text{(B14)}\qquad \mu\,\frac{\sin(\phi+\alpha-\gamma)}{\cos(\alpha-\gamma)} + \mu^{\frac{q-2}{2}}\,\mathrm{Im}(Ce^{-iq\theta}) = 0.$$

Since

$$\mathrm{Im}(Ce^{-iq\theta}) \leq C$$

this means an inequality of the kind

(B15) $$|\sin(\phi+\alpha-\gamma)| \leq A\mu^{q/2-2}.$$

The region determined by (B15) is sketched below. Obviously it is horn-shaped with the axis $\phi = \gamma-\alpha$

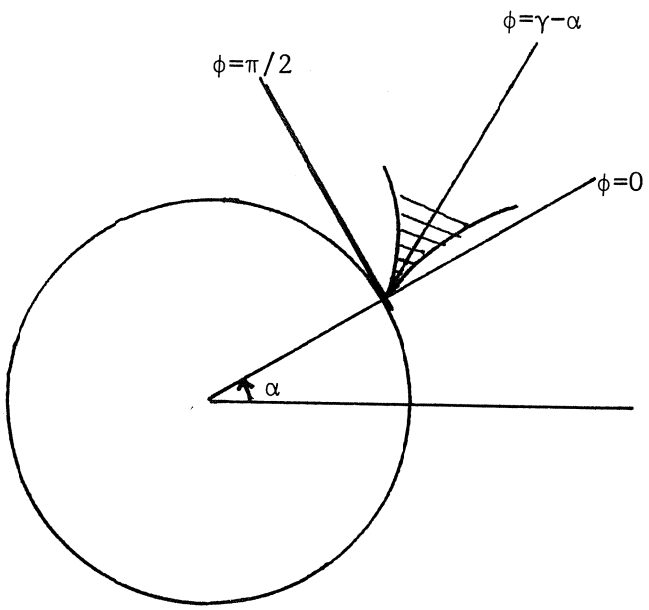

It is perhaps of some practical interest to consider the special case with q = 5 in somewhat more detail. The normal form is given by (A7) as

(B16) $$w = \lambda z - Qz^{2-}\bar{z} + Cz^{-4} \ldots .$$

By a similarity transformation it can be arranged that C = 1. In polar coordinates we obtain with

$$w = r' \exp i\theta', \quad z = r \exp i\theta$$

$$\text{(B17)} \qquad \begin{cases} r'^2 = r^2(1+2\mu\cos\phi-2c\cos(\alpha-\gamma)r^2+2r^3\cos(5\theta+\alpha)) + \dots , \\ \theta' = \theta + \alpha + \mu\sin\phi - c\sin(\alpha-\gamma)r^2 - r^3\sin(5\theta+\alpha) + \dots . \end{cases}$$

The conditions for a cycle of period 5 are

$$\text{(B18)} \qquad \begin{cases} \mu\cos\phi - cr^2\cos(\alpha-\gamma) + r^3\cos(5\theta+\alpha) = 0, \\ \mu\sin\phi + cr^2\sin(\alpha-\gamma) - r^3\sin(5\theta+\alpha) = 0. \end{cases}$$

If $\cos(\alpha-\gamma) > 0$ there exists a Hopf radius $r = R$ given by (B12) which solves the first equation of (B18) in the lowest order approximation. From (B18) we obtain by eliminating the middle terms

$$\text{(B19)} \qquad r^3\sin(5\theta+\gamma) = \mu\sin(\phi+\alpha-\gamma).$$

If $r = R$ a value of 5θ can be obtained only if

$$\text{(B20)} \qquad R^3 \geq \mu\sin(\phi+\alpha-\gamma),$$

which is in fact Arnold's horn condition. In local coordinates $x = \mu\cos\phi$, $y = \mu\sin\phi$ this can be written as

$$\text{(B21)} \qquad x^3 \geq c^3\cos^3(\alpha-\gamma)(x\sin(\alpha-\gamma)+y\cos(\alpha-\gamma))^2$$

being the equation of a cubic parabole with the axis

$$\text{(B22)} \qquad x\sin(\alpha-\gamma) + y\cos(\alpha-\gamma) = 0.$$

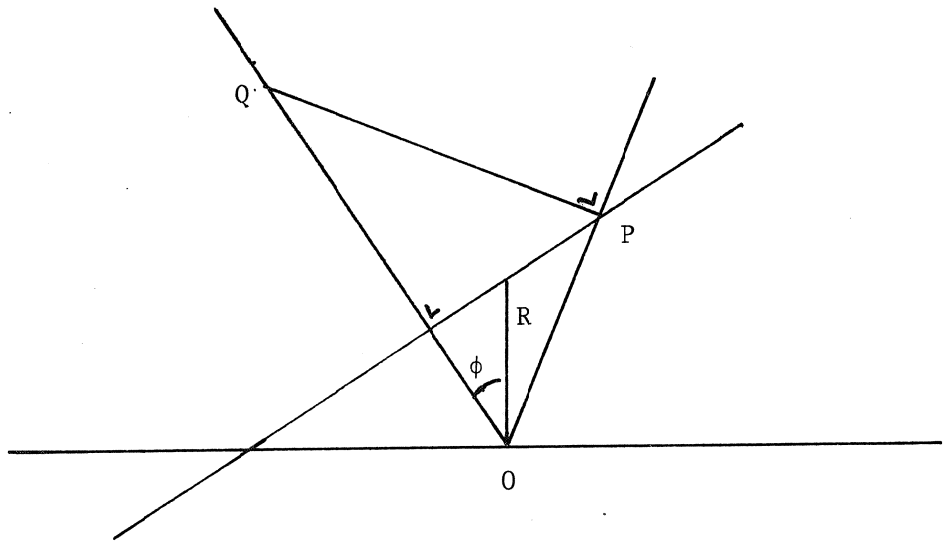

The formulae given above lead to the following geometrical construction. Let in the complex plane Q be the image of c exp iγ and let the line OP indicate the angle α. Then take P and R such that ∠ OPQ = π/2 and PR⊥OQ. If ∠ QOR = φ then PR is the Hopf radius in the critical situation on the boundary of Arnold's horn. This statement follows easily by applying the sine rule in ΔOPR

$$\frac{PR}{|\sin(\gamma-\alpha-\phi)|} = \frac{c\cos(\gamma-\alpha)}{\cos\phi}.$$

Appendix C

In this section we determine the shape of the Hopf ellipse of the planar map

$$(C1) \qquad \begin{cases} x' = y \\ y' = Ax + By + Cx^2 + Dxy + Ey^2 \end{cases}$$

at the critical eigenvalue

$$\lambda = (1+\mu)e^{i\alpha}, \quad 0 < \alpha < \pi. \tag{C2}$$

Of course

$$A = -\lambda\bar{\lambda}, \quad B = \lambda + \bar{\lambda}. \tag{C3}$$

The first task is to bring (C1) into the pre-normal form (A1). This can be effected by the linear transformation, written in complex form as

$$z = ix\bar{\lambda} - iy \tag{C4}$$

and in real form as

$$\begin{cases} \xi = (1+\mu)x \sin\alpha, \\ \eta = (1+\mu)x \cos\alpha - y, \end{cases} \tag{C5}$$

where $z = \xi + i\eta$.
The result is

$$w = \lambda z + A_2(z,\bar{z}) \tag{C6}$$

where

$$iA_2(z,\bar{z}) = Cx^2 + Dxy + Ey^2 \tag{C7}$$

with

$$\begin{cases} (\lambda-\bar{\lambda})x = i(z+\bar{z}), \\ (\lambda-\bar{\lambda})y = i(\lambda z+\bar{\lambda}\bar{z}). \end{cases} \tag{C8}$$

For the calculation of the Hopf radius according to (B8) we need only the coefficients of $A_2(z,\bar{z})$ for $\mu = 0$. This means that λ may be replaced by

exp iα. In this way we obtain

$$(C9)\qquad \begin{cases} 4ia_{20}\sin^2\alpha = C + \lambda D + \lambda^2 E, \\ 4ia_{11}\sin^2\alpha = 2C + (\lambda+\bar{\lambda})D + 2E, \\ 4ia_{02}\sin^2\alpha = C + \bar{\lambda}D + \bar{\lambda}^2 E. \end{cases}$$

Substitution of these expressions in (B8) gives

$$(C10)\qquad \frac{16\mu\sin^4\alpha}{R^2} = 3F^2 + G\sin^2\alpha + ((4\cos^2\alpha-2\cos\alpha-3)C+(2\cos\alpha-1)D+3E)F,$$

where

$$(C11)\qquad F = C + D\cos\alpha + E,$$

and

$$(C12)\qquad G = D^2 - 4CE.$$

The equation of the invariant Hopf circle $z\bar{z} = R^2$ in the original variables can be obtained from (C4) as

$$(x\lambda-y)(x\bar{\lambda}-y) = R^2$$

or

$$(C13)\qquad x^2 - 2xy\cos\alpha + y^2 = R^2.$$

Thus for (C1) we have a Hopf ellipse with semi-axes

$$(C14)\qquad \frac{R}{\sqrt{2}\sin\alpha/2}\ ,\quad \frac{R}{\sqrt{2}\cos\alpha/2}\ .$$

REFERENCES

[1] POUNDERS, J.R. & Th. D. ROGERS (1982), *The geometry of chaos: Dynamics of a nonlinear second-order difference equation*. Bull. Math. Biology, 42, 551-597.

[2] ARONSON, D.G. et al. (1982), *Bifurcation from an invariant circle for two-parameter families of maps of the plane. A computer assisted study*. Comm. Math. Phys. 3, 303-354.

[3] LAUWERIER, H.A. (1983), *Bifurcation of a map at resonance* 1 : 4. Report TW 245, Mathematisch Centrum, Amsterdam.

[4] ARNOLD, V.I. (1983), *Geometrical methods in the theory of ordinary differential equations*. (Translation of "Supplementary Chapters of the theory of o.d.e.'s".) Springer, Grundlehren vol. 250.

[5] IOOSS, G. (1979), *Bifurcation of maps and applications*. North Holland, Mathematics Studies vol. 36.

[6] WHITLEY, D. (1983), *Discrete dynamical systems in dimensions one and two*. Bull. Lond. Math. Soc. 15, 177-217.